Time Evolution of NMR Proton Chemical Shifts of an RNA Hairpin during a Molecular Dynamics Simulation

Jacek Nowakowski,[§] Jennifer L. Miller,[†] Peter A. Kollman,[†] and Ignacio Tinoco, Jr.*[,§]

Contribution from the Department of Chemistry, University of California, Berkeley and Structural Biology Division, Lawrence Berkeley National Laboratory, Berkeley, California 94720-1460, and Department of Pharmaceutical Chemistry, University of California, San Francisco, California 94143

Received July 26, 1996[⊗]

Abstract: We have calculated the time evolution of three nonlocal contributions to the proton chemical shifts of a ribonucleic acid: ring current effects, intramolecular electrostatic shifts, and electrostatic shifts due to solvent. The computation was done on a 1.075 ns molecular dynamics trajectory of a fully solvated RNA hairpin with sodium counterions. The calculated shift components exhibit rapid fluctuations on a subpicosecond time scale. The magnitudes of fluctuations are dependent on two factors: the proximity of a shift source and the dynamics of the local RNA structure. The largest fluctuations were found for the shifts of exchangeable protons due to the electrostatic effects of hydrogen bond acceptors. The magnitudes of the time-averaged shifts differ significantly for the ring current and intramolecular electrostatic contributions in a structure-dependent manner. For the ribose and exchangeable aromatic protons, the major contributor to the total chemical shift is the intramolecular electrostatic effect, whereas nonexchangeable aromatic proton shifts are equally affected by ring current effects and intramolecular electrostatic shifts. Changes in the ribose sugar pucker cause large changes in the nonlocal contributions to the chemical shifts of the H2′, H3′, and H4′ protons. Empirical values of local chemical shifts provided good agreement between calculated and measured shifts for the nonexchangeable aromatic protons when the solvent contributions were excluded from the calculation.

Introduction

It has been long recognized that NMR chemical shifts carry useful structural information about molecules and their surroundings. In the field of structural biology, chemical shifts of ^{1}H, ^{13}C, ^{15}N, ^{31}P nuclei can be used to improve the quality of structures of nucleic acids and proteins.[1−5] Although the accurate calculation of absolute chemical shifts are not yet possible for large molecules, there are several well-established approximations for calculating nonlocal contributions to the chemical shift.[6−9] These methods have been successfully used to both model and refine biomolecular structures.[10−12]

It is generally assumed that the total chemical shift of a nucleus in a biopolymer can be expressed as[2,13]

$$\delta = \delta_d(\text{local}) + \delta_p(\text{local}) + \delta_{rc} + \delta_{el} + \delta_{ma} + \delta_{sol} \quad (1)$$

where δ_d(local) and δ_p(local) are the diamagnetic and paramagnetic terms which incorporate the effect of the local electron distribution around the nucleus. The nonlocal effects are δ_{rc}, the ring current shift of aromatic rings present in the molecule, δ_{el}, intramolecular electrostatic effects, δ_{ma}, magnetic anisotropy of distant bonds or groups (e.g. peptide bonds in proteins), and δ_{sol}, the shift induced by the solvent. The last four terms in eq 1 can be used to gain insight into the molecular structure, because of their dependence on long-distance through-space interactions. In reality, chemical shifts measured in NMR experiments are time-averaged over a multitude of dynamic motions which occur on a subpicosecond to millisecond time scale. Understanding these averaging processes is important to accurately use the chemical shifts in structure analysis and refinement. Molecular dynamics simulations are ideally suited for such investigations since they provide a detailed picture of molecular and solvent fluctuations on a nanosecond time scale from which the time dependence of chemical shifts can be calculated.[14−16]

In this report, we compute the time evolution of three nonlocal contributions to the proton chemical shift of an RNA hairpin: the ring current effect (δ_{rc}), the intramolecular electrostatic shift (δ_{el}), and the electrostatic shift due to water and sodium counterions (δ_{sol}). RNA and DNA molecules contain many aromatic residues, their backbones are highly charged, and many

[§] Department of Chemistry, University of California, Berkeley and Structural Biology Division, Lawrence Berkeley National Laboratory, Berkeley, California.

[†] Department of Pharmaceutical Chemistry, University of California, San Francisco.

[⊗] Abstract published in *Advance ACS Abstracts,* December 1, 1996.

(1) Wishart, D. S.; Sykes, B. D.; Richards, F. M. *Biochemistry* **1992**, *31*, 1647−1651.
(2) de Dios, A. C.; Pearson, J. G.; Oldfield, E. *Science* **1993**, *260*, 1491−1496.
(3) Oldfield, E. *J. Biomol. NMR* **1995**, *5*, 217−225.
(4) Spera, S.; Bax, A. *J. Am. Chem. Soc.* **1991**, *113*, 5490−5492.
(5) Wishart, D. S.; Sykes, B. D. *J. Biomol. NMR* **1994**, *4*, 171−180.
(6) Johnson, C. E., Jr.; Bovey, F. A. *J. Chem. Phys.* **1958**, *29*, 1012−1014.
(7) Buckingham, A. D. *Can. J. Chem.* **1960**, *38*, 300−307.
(8) Haigh, C. W.; Mallion, R. B. *Prog. NMR Spectrosc.* **1980**, *13*, 303−344.
(9) McConnell, H. M. *J. Chem. Phys.* **1957**, *27*, 226−229.
(10) Ösapay, K.; Case, D. A. *J. Biomol. NMR* **1994**, *4*, 215−230.
(11) Ösapay, K.; Theriault, Y.; Wright, P. E.; Case, D. A. *J. Mol. Biol.* **1994**, *244*, 183−197.
(12) Le, H.-b.; Pearson, J. G.; de Dios, A. C.; Oldfield, E. *J. Am. Chem. Soc.* **1995**, *117*, 3800−3807.
(13) Ösapay, K.; Case, D. A. *J. Am. Chem. Soc.* **1991**, *113*, 9436−9444.
(14) Hoch, J. C.; Dobson, C. M.; Karplus, M. *Biochemistry* **1982**, *21*, 1118−1125.
(15) Svishchev, I. M.; Kusalik, P. G. *J. Am. Chem. Soc.* **1993**, *115*, 8270−8274.
(16) Lau, E. Y.; Gerig, J. T. *J. Am. Chem. Soc.* **1996**, *118*, 1194−1200.

S0002-7863(96)02594-2 CCC: $12.00

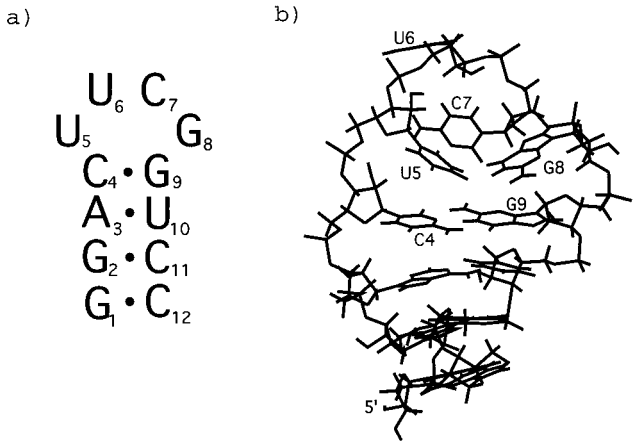

Figure 1. Secondary (a) and tertiary (b) structure of the UUCG RNA hairpin. The tertiary structure is from ref 30.

protons are generally accessible to the solvent. Thus, it is likely that these three terms are the main contributors to the nonlocal proton chemical shifts in nucleic acids.[17] The magnetic anisotropy effects of phosphates and ribose groups were omitted from our calculation, because the anisotropy of the magnetic susceptibility tensor for single bonds is generally small,[18] and phosphates have an approximate spherical symmetry. As a model molecule, we chose an ultrastable 5′GGAC(UUCG)-GUCC RNA hairpin whose structure has been determined at high resolution from NMR studies (Figure 1).[19,20] A high quality, molecular dynamics trajectory has been recently computed for this molecule using the particle mesh Ewald (PME) method for the treatment of long-range electrostatic interactions.[21] This stable trajectory of fully solvated, fully charged RNA in a nanosecond time range provided us with a state-of-the-art description of RNA dynamics in solution.

To obtain the time evolution of proton chemical shifts, we computed the shift components from atomic coordinate snapshots collected every picosecond. We used the Johnson−Bovey equation[6,8,22,23] for evaluating the ring current effect and Buckingham's formalism[7,13,15,24] for both intramolecular and solvent electrostatic effects. The computational parameters used in the shift calculations were obtained from the best least squares fit of calculated values to measured chemical shifts for the aromatic protons. The purpose of this investigation is to assess the extent of motional averaging and the relative magnitudes of the main contributions to the chemical shift. In the following sections we present discussion of the dependence of calculated chemical shifts on RNA structure and dynamics.

Computational Methods

The molecular dynamics trajectory of the UUCG RNA hairpin was computed using program AMBER 4.1 with the Cornell et al.[25] force field. The simulation was run for a total time of 1.075 ns at 300 K with the particle mesh Ewald (PME) method for treatment of long-range electrostatic effects. The simulation system consisted of RNA (12 nucleotides, 382 atoms), 2154 water molecules, and 11 sodium ions in a 47.0 × 44.0 × 39.0 Å^3 box.[21] Chemical shifts for all RNA protons were calculated from atomic coordinates obtained every 1 ps, totaling 1075 sets of values. The ring current effect (RC) was calculated using the Johnson−Bovey approximation.[6] In this method the shift is expressed as

$$\delta_{rc} = iBG(r) \tag{2}$$

where $G(r)$ is a geometric factor which represents the magnetic field of circles of current above and below each aromatic ring, B incorporates the ring current of a benzene, and i is the current intensity factor for a specific aromatic ring. The form of the geometric factor $G(r)$ is given in Giessner-Prettre et al.[23] We used the values of B and i recently calibrated for nucleic acid bases by Case.[26] The ring current calculation for ribose protons included effects of all aromatic rings; the calculation for aromatic protons included the effects of all other bases.

The intramolecular electrostatic shift due to RNA (EL) and solvent atoms (SOL) were determined using Buckingham's formalism.[7] In this approach chemical shift induced in a proton by an external electric field is

$$\delta_{el} = AE_{bond} \tag{3}$$

where E_{bond} is the component of the total external electric field, **E**, along the proton bond and $A = -2.98 \times 10^{-12}$ esu^{-1} cm^2 is the shielding polarizability.[26,27] Although this expression represents only the first term in an expansion, the higher order terms were generally small and were excluded from the computational procedure.[24,26] The **E** vector is calculated from atomic partial charges q_{atom} using Coulomb's law

$$\mathbf{E} = \sum_{\text{residues}} \sum_{\text{atoms}} \frac{q_{\text{atom}}\hat{\mathbf{r}}}{\epsilon r^2}$$

where r is the distance between the charge and the nucleus and $\hat{\mathbf{r}}$ is a unit vector from the charge to the nucleus. We used AMBER[25] partial charges on RNA atoms, TIP3P[28] charges on water, and +1 charges on sodium counterions. The calculations of intramolecular and solvent electrostatic effects were done with two common models of the dielectric function: distance-dependent ($\epsilon = \alpha r$) and distance-independent ($\epsilon = \alpha$). The value of α was determined by best least squares fitting to experimental data. The electrostatic shift calculated for ribose and aromatic protons excluded the effects of atoms in their own group.

In the following discussion we label the individual protons with the name of the proton first and residue type and number second (e.g. H8 A3 indicates proton H8 of the third adenine). The numbering of nucleotide protons is shown in Figure 2.

Results

A. Calibration of the Computational Parameters and Comparison with Experiment. Direct comparison of our calculations with experiment is impossible since only the nonlocal *contributions* to the chemical shifts are computed. In order to obtain the total shift, the local terms δ_d(loc) and δ_p-(loc) need to be known for different RNA protons as a function of conformation. These values can be either obtained by *ab initio* quantum mechanical calculations or fitted empirically to measured shifts for a large number of known high-resolution RNA structures. In proteins, the local terms of proton shifts have been obtained for individual amino acids from shifts measured in small peptides and calibrated against a large number of crystal structures.[13] This approach assumes that short peptides are structurally disordered and that most of the nonlocal

(17) Giessner-Prettre, C.; Pullman, B. *Q. Rev. Biophys.* **1987**, *20*, 113−172.
(18) Flygare, W. H. *Chem. Rev.* **1974**, *74*, 653−687.
(19) Cheong, C.; Varani, G.; Tinoco, I., Jr. *Nature* **1990**, *346*, 680−682.
(20) Allain, F. H.-T.; Varani, G. *J. Mol. Biol.* **1995**, *250*, 333−353.
(21) Cheatham, T. E. I.; Miller, J. L.; Fox, T.; Darden, T. A.; Kollman, P. A. *J. Am. Chem. Soc.* **1995**, *117*, 4193−4194.
(22) Perkins, S. J.; Dwek, R. A. *Biochemistry* **1980**, *19*, 245−258.
(23) Giessner-Prettre, C.; Pullman, B. *Biopolymers* **1976**, *15*, 2277−2286.
(24) Williamson, M. P.; Asakura, T. *J. Magn. Reson. Ser. B* **1993**, *101*, 63−71.
(25) Cornell, W. D.; Cieplak, P.; Bayly, C. I.; Gould, I. R.; Merz, K. M.; Ferguson, D. M.; Spellmeyer, D. C.; Fox, T.; Caldwell, J. W.; Kollman, P. A. *J. Am. Chem. Soc.* **1995**, *117*, 5179−5197.
(26) Case, D. A. *J. Biomol. NMR* **1995**, *6*, 341−346.
(27) Augspurger, J. D.; Dykstra, C. E. *J. Phys. Chem.* **1991**, *95*, 9230−9238.
(28) Jorgensen, W. L.; Chandrasekhar, J.; Madura, J. D. *J. Chem. Phys.* **1983**, *79*, 926−935.

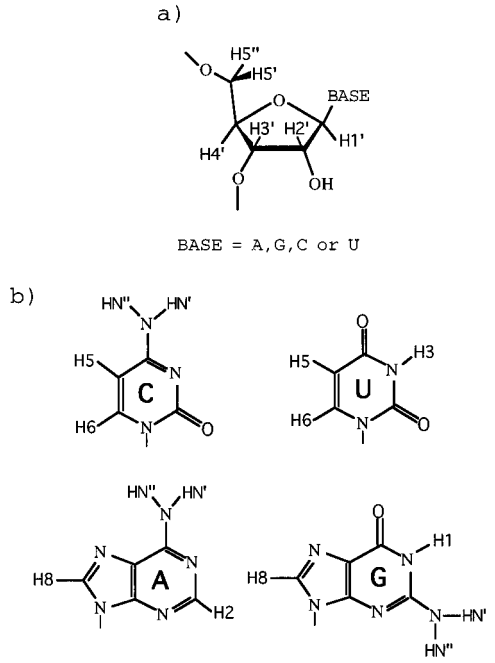

Figure 2. Proton nomenclature for ribose (a) and RNA bases (b).

terms average to zero. Unfortunately, nucleic acids are known to have a significant amount of structural order even for di- and trinucleotides due to base stacking.[29] Therefore this method cannot be easily applied to RNA and DNA molecules. At present the number of high resolution structures of RNA is also very small.

The local terms for exchangeable protons are strongly dependent on hydrogen bonding, and those for ribose protons depend on each individual sugar pucker. These values will be different for the same proton in different nucleotides depending on the local conformation. On the other hand, δ_d(loc) and δ_p(loc) should be nearly constant for the nonexchangeable aromatic protons on effectively rigid bases. It is thus possible to obtain local shifts for the aromatic protons by finding the best fit to the experimental data of the shifts calculated with eq 1. This approach can also be used to calibrate the value of the dielectric constant in the calculation of electrostatic contributions.

The UUCG hairpin contains 20 nonexchangeable aromatic protons which can be represented by seven types: AH2, AH8, GH8, CH5, CH6, UH5, UH6. In order to find the local shift contributions for these classes of protons, the calculated values of δ_{rc}, δ_{el}, and δ_{sol} were used in the best least squares fit of the equation

$$\delta_{total} = \delta_{loc} + B_{rc}\delta_{rc} + A_{el}\delta_{el} + C\delta_{sol} \qquad (5)$$

to the measured chemical shifts.[30] The parameters δ_{loc} are the local shifts of the seven types of protons. The parameters A_{el} and C combine the value of the Buckingham parameter A in eq 3 and the inverse of the parameter α in the dielectric constant used in the calculation of intramolecular and solvent electrostatic contributions. We have used two different sets of calculated electrostatic contributions obtained with $\epsilon = 1$ and $\epsilon = r$ to test two models of dielectric function commonly used in calculations of electric fields in biomolecular systems.[31] Various combinations of parameters A_{el} and C were tested. The best fit between the calculated and measured shifts was found for the intramolecular electrostatic shifts calculated with the distance independent form of dielectric function ($\epsilon = 1$) and by setting $C = 0$, which excluded the solvent contribution. The results of the best fit procedure are given in Table 1, and the agreement between calculated and measured shifts is shown in Figure 3. The fit is reasonable with a standard deviation of 0.13 ppm.

(29) Lee, C.-H.; Tinoco, I., Jr. *Biophys. Chem.* **1980**, *11*, 283−294.
(30) Varani, G.; Cheong, C.; Tinoco, I., Jr. *Biochemistry* **1991**, *30*, 3280−3289.
(31) Warshel, A.; Russel, S. T. *Q. Rev. Biophys.* **1984**, *17*, 283−422.

Table 1. Computational Parameters Obtained from the Best Least Square Fit of Eq 5 to the Measured Shifts of Nonexchangeable Aromatic Protons

δ_{loc}									
G H8	C H6	C H5	U H6	U H5	A H8	A H2	B_{rc}	A_{el}	C
8.08	7.56	5.95	7.83	5.86	8.27	7.78	1.056	0.474	0.00

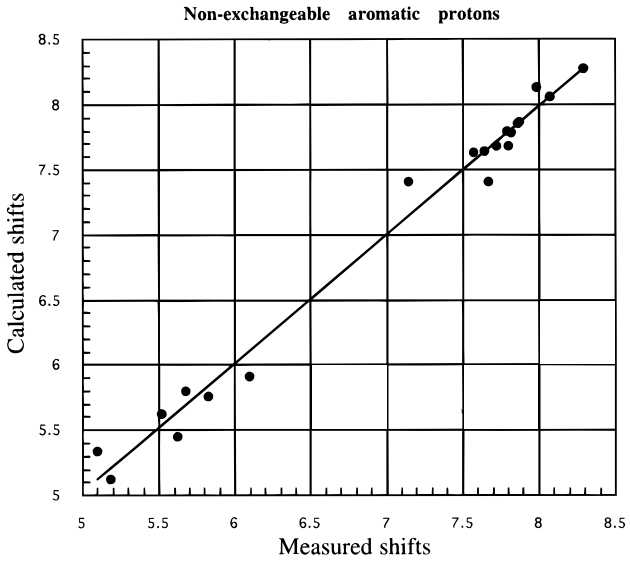

Figure 3. Plot of measured vs calculated chemical shifts for the 20 nonexchangeable aromatic protons in UUCG hairpin. The shifts were calculated with 10 parameters obtained from the best least square fit to the measured values. The line is given by $y = 0.0958 + 0.986x$, $R = 0.993$. The standard deviation between calculated and measured chemical shifts is 0.13 ppm.

In the following discussion of the time evolution of chemical shifts we used the values of shifts calculated with parameters given in Table 1. Since the magnitude of solvent contribution cannot be reliably evaluated for protons other than those used in the fitting procedure, we avoided comparisons of the scale of this effect with RC and EL contributions. We expect that solvent electrostatic effects will be significant for the exchangeable protons (which were not included in the calibration procedure). To qualitatively illustrate the time-evolution of this contribution, we calculated the magnitude of the solvent effect with $\epsilon = r$.

B. General Features. The time evolution of RNA proton chemical shifts reveals high frequency fluctuations in magnitude due to fast motions of the molecule and the surrounding solvent (Figure 4 a−d, left panels). The values of shifts calculated from consecutive snapshots ($\Delta t = 1$ ps) differ by as much as 0.2 ppm indicating that the chemical shifts are very susceptible to even small changes in structure which occur on a subpicosecond time scale. The majority of shifts oscillate around a single time-average value different for each proton. The most notable exceptions are the shifts of protons caused by the change in sugar pucker (between 3′-endo and 2′-endo) of residue C12. The different ribose conformations cause the protons to have two distinctly different average values (Figure 4d, for details see part E, this section). The values of calculated shifts are characterized by a nearly normal distribution around the mean value (Figure 4, right panels) with the spread corresponding to the amplitude of oscillations.

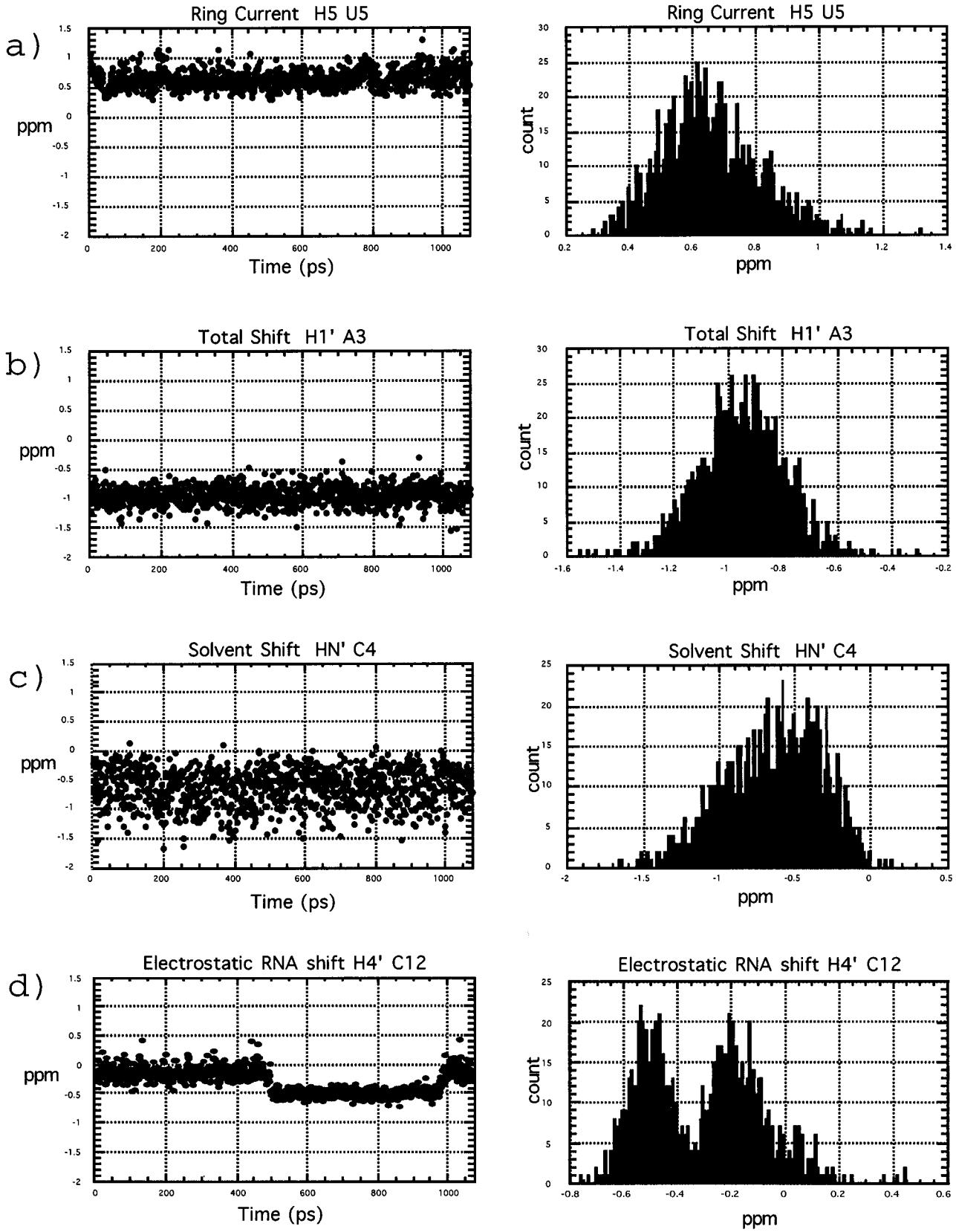

Figure 4. Left panels: chemical shift fluctuations as a function of time for (a) ring current of H5 U5, (b) total shift (RC + EL + SOL) of H1′ A3, (c) solvent shift of HN′ C4, and (d) intramolecular electrostatic shift of H4′ C12. Right panels: distributions of shift values calculated from 1075 molecular dynamics snapshots. H4′ C12 is involved in a ribose puckering and shows two different time-averaged shift values.

The shift fluctuations originating from RNA dynamics and solvent motions on the nanosecond time scale range from 2.51 to 0.10 ppm (Table 2). On average, these differences are much smaller than the values previously reported in a protein simulation where oscillations as large as 6 ppm were found for the ring current shifts.[14] We find that the magnitude of fluctuation is generally dependent on two factors: flexibility of the particular region of RNA structure and the magnitude of the average shift value. Large shifts which are induced by close proximity of the shift source are extremely sensitive to even small changes in structure. Figure 5 illustrates this effect. Proton H5 of U10 (Figure 5a) in the UUCG structure is close

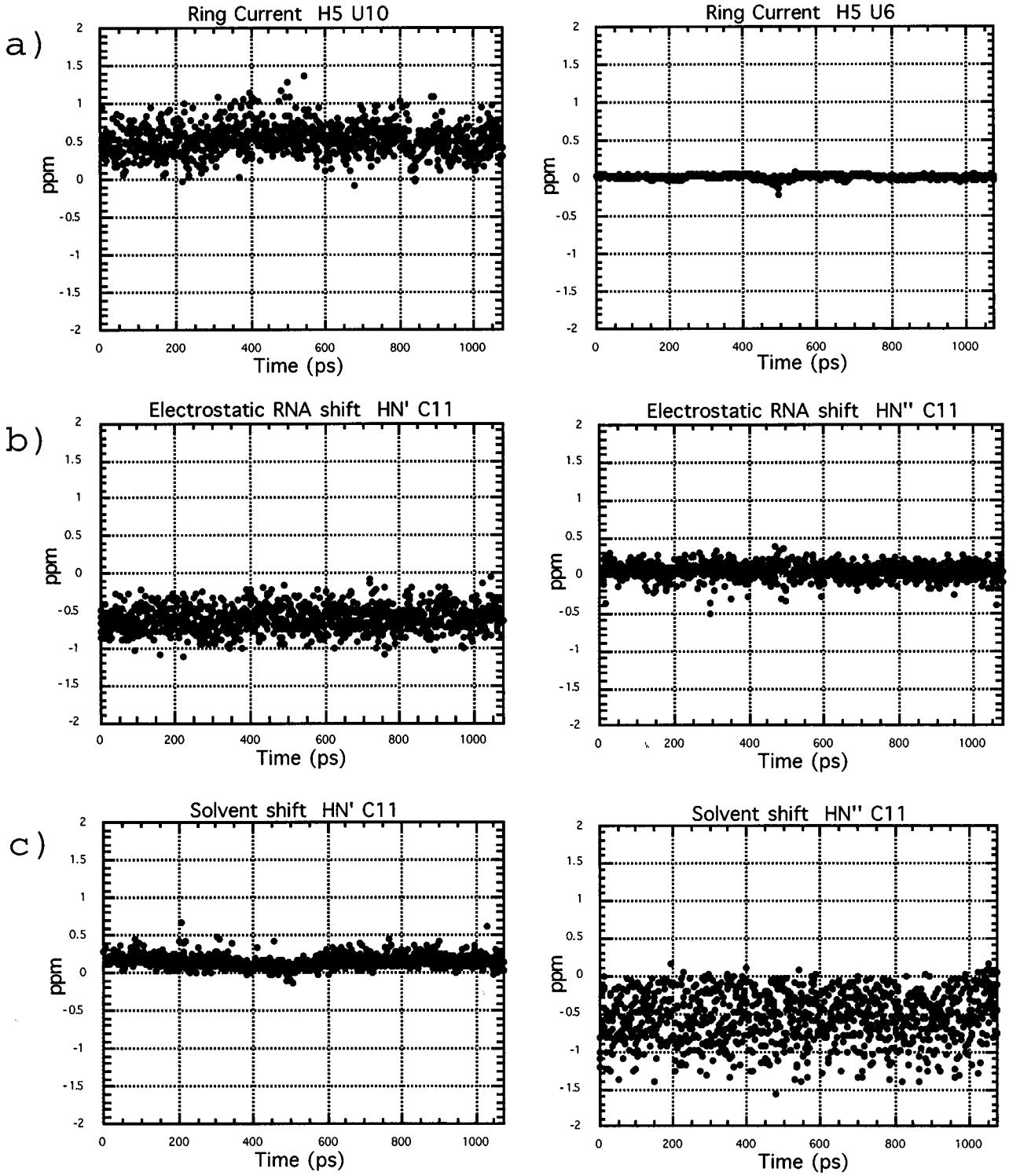

Figure 5. Dependence of the magnitude of shift fluctuations on the dynamics, location, and type of RNA protons. Time plots of ring current shift of H5 U10 (a, left panel) and H5 U6 (a, right panel). Plots of intramolecular electrostatic shifts (b) and solvent shifts (c) of amino protons of residue C11.

to the aromatic rings of G9, C11, and A3 and exhibits a large ring current effect (0.53 ppm). Although U10 is not very flexible because it belongs to the structured, double helical stem, the ring current shift of H5 proton shows large fluctuations. On the other hand, the ring current shift of H5 U6 fluctuates very little despite the fact that this nucleotide is the most dynamic part of the hairpin (Figure 5a, right panel). Since this proton is exposed to the solvent and located far away from other aromatic rings even a large amplitude of motion does not have a significant effect on the induced shift. The same effects are true for electrostatic shifts. Figure 5b,c show the amino protons of residue C11. This nucleotide is base paired with G2 through a standard Watson−Crick geometry. The HN′ proton is part of the hydrogen bond network, and its intramolecular electrostatic shift fluctuates significantly because of the close proximity of the negative partial charge of O6 G2. The same proton is protected from the solvent, and therefore the electrostatic shift due to water and sodium counterions is small and shows little variation in time (Figure 5b, right panel). The opposite situation is found in the time evolution of the electrostatic shifts for the HN″ proton, which is solvent exposed but not internally hydrogen bonded (Figure 5c).

Table 2. Ranges of Calculated Time-Averaged Shift Values[a] and Magnitudes of Shift Fluctuations

		total shift ($\delta_{rc} + \delta_{el}$)	RC shift (δ_{rc})	El RNA shift (δ_{el})
range of av values (ppm)	min.	−1.32 (G1 H2′)[b]	−0.68 (A3 H1′)	−1.05 (G1 H2′)
	max.	1.04 (G8 H8)	1.06 (G8 H1)	0.33 (G2 HN″)
range of fluctuations (Δ ppm)	min.	0.33 (G4 H4′)	0.10 (C11 H5′)	0.27 (G8 H8)
	max.	2.51 (G2 H1)	2.26 (G2 H1)	1.63 (C7 HN′)

[a] Positive shift value indicates shielding (upfield) and negative value deshielding. [b] The name of the proton in parentheses corresponds to the calculated value.

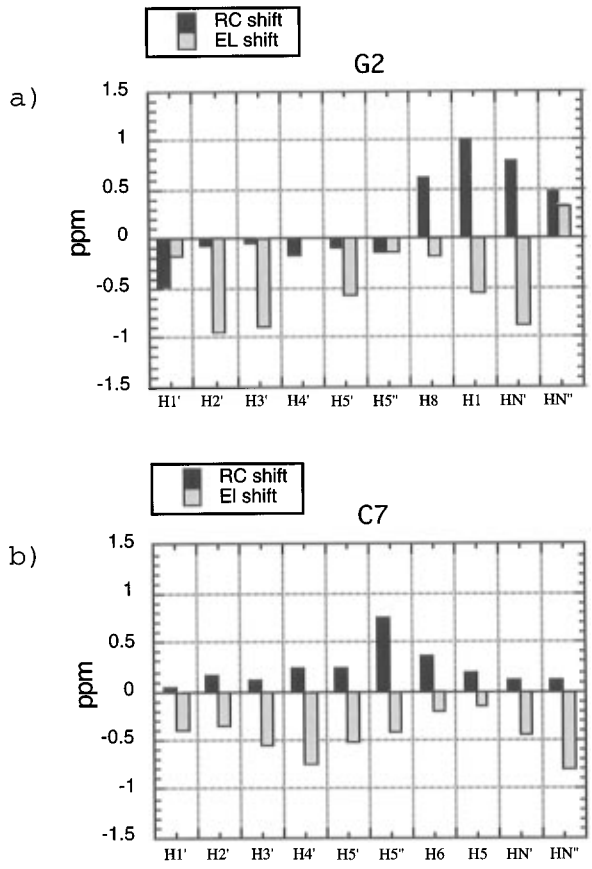

Figure 6. Relative magnitudes of the ring current (RC shifts) and intramolecular electrostatic (EL shift) shifts for protons of residues G2 and C7. Residue G2 is representative of a nucleotide in a standard A-form helix environment. C7 illustrates magnitudes of shift contributions for a nonstandard geometry.

C. Magnitudes of Individual Shift Contributions. The ring current (RC) and intramolecular electrostatic (EL) shift contributions vary significantly in their magnitudes in a structure-dependent manner. In a regular duplex region (nucleotides G1-C4 and G9-C12), the magnitude of the ring current shift is largest for protons closest to aromatic rings: aromatic protons and ribose H1′s (Figure 6a). For the loop nucleotides (residues U5-G8) the magnitude of the RC shift depends on the local geometry (Figure 6b). For instance, the H5″ proton of C7 experiences a large RC shielding shift of 0.75 ppm due to the closeness of the G8 aromatic ring. The measured chemical shift of this residue is 2.74 ppm, which is about 1.3 ppm upfield from the average shift of H5″ protons in RNA.[30] Our calculation shows that the origin of this unusual shift is mainly due to the ring current effect. The RC shifts can be both shielding and deshielding depending on the spatial orientation of the proton with respect to the plane of aromatic bases (Table 2). The intramolecular electrostatic RNA shifts are deshielding for 66 out of 72 ribose protons and for most of the aromatic protons (34/48). The largest deshielding shifts are seen for hydrogen-bonded exchangeable protons due to the close proximity of negatively charged hydrogen bond acceptor atoms.

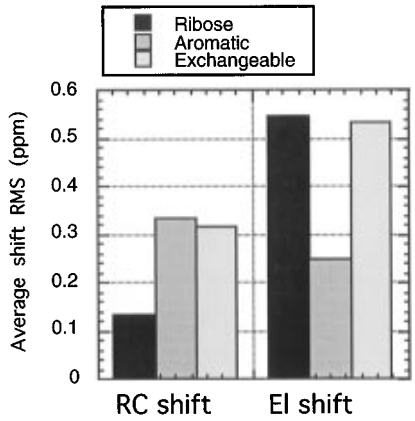

Figure 7. Average root mean square values of the ring current (RC shifts) and intramolecular electrostatic (EL shifts) shift components for the three structurally distinct proton groups: ribose protons (black), aromatic nonexchangeable protons (gray), and aromatic exchangeable protons (light gray).

The magnitudes of EL shifts are significant for protons in both the loop and the stem regions (Figure 6).

Figure 7 compares the average root mean square magnitudes of the ring current and intramolecular electrostatic shift contributions for three structurally distinct groups of hydrogens: ribose protons (H1′−H5″), aromatic nonexchangeable protons (H6, H5 of pyrimidines and H8, H2 of purines), and aromatic exchangeable protons (imino and amino protons). For the ribose protons, which are on average far from aromatic bases and nonaccessible to the solvent, the major contributor to the total chemical shift is the intramolecular electrostatic effect. For the nonexchangeable aromatic protons the most significant contributions are both the ring current effect and intramolecular electrostatic shift. Finally, the shifts of exchangeable aromatic protons are dominated by the electrostatic contribution. The solvent electrostatic shift calculated with $\epsilon = r$ also has a significant effect on non-hydrogen bonded exchangeable protons. The magnitude of this effect can be as large as the ring current shift (data not shown).

D. Time-Averaged Shifts versus Average Structure Shifts and NMR Structure Shifts. During the molecular dynamics simulation the transient RNA structures deviate from the NMR-derived structure as they evolve in time. The shift components calculated from these intermediate set of coordinates represent the correct time-averaged chemical shifts. In order to assess the effects of the averaging process on the magnitude of individual shift components, we compared the time-averaged shifts with shifts computed directly from the NMR-derived structure and with shifts calculated from the average structure obtained from the entire trajectory. The left panels of Figure 8 shows that time-averaged ring current contributions are almost identical with shifts calculated from the average structure. The correlation is less perfect for the intramolecular electrostatic shift (Figure 8c), but the agreement is still good. On the other hand, the correlation between the time-averaged shifts and shifts computed from the NMR-derived structure is much worse (Figure 8, right panels). The discrepancy is especially large

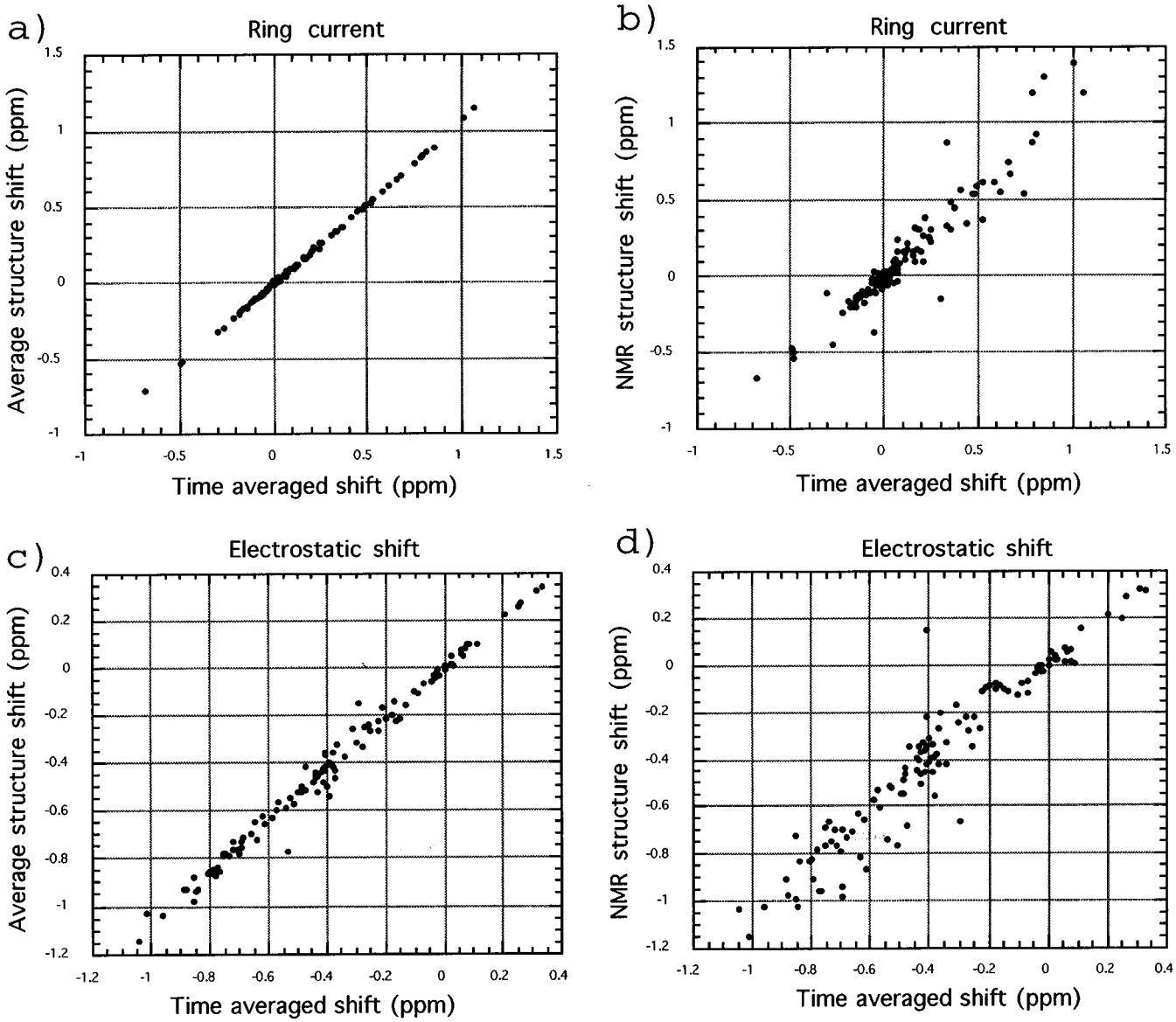

Figure 8. Plots of time-averaged ring current shifts (top panels) and intramolecular electrostatic shifts (bottom panels) against shifts calculated from (a,c) average coordinates structure and (b,d) energy-minimized NMR structure. Standard deviations for plots are (a) 0.019, (b) 0.117, (c) 0.044, (d) 0.123 ppm.

for large magnitudes of ring current and intramolecular electrostatic shifts. Out of 120 shifts compared, 10% of RC and 16% of EL RNA shifts differed by more than 0.2 ppm. These findings imply that time-averaged chemical shifts can be approximated by shifts computed from the average structure but cannot be reproduced reliably from a single energy-minimized NMR structure.

E. Effects of Sugar Puckering on Chemical Shifts. The ribose of the terminal cytosine residue C12 undergoes a reversible conformational change from C3′ endo (N) to C2′ endo (S) sugar pucker (for nomenclature see Saenger[32]) during the simulation. The ring flip occurs at 480 ps, the new conformation is retained for 500 ps, and the reverse puckering occurs at 980 ps. The occurrence of this event in the molecular dynamics simulation is in agreement with the experimental NMR data which shows that the ribose of the C12 is in a conformationally mixed state.[30] The change in sugar pucker involves spatial rearrangement of several backbone atoms and H2′, H3′ and to a smaller extent H4′ protons. As expected, these hydrogens experience a change in calculated chemical shifts during the transition. The time evolution plots of shift components for these protons show distinctly different average shift values for 0−480 and 480−980 ps time periods (Figures 9 and 4d). In several instances the change in the average shift value is also accompanied by a new magnitude of shift fluctuation. For example, the RC shift of C12 H3′ oscillates as much as 0.3 ppm during the C3′ endo conformation, but the switch in the pucker reduces the fluctuations to 0.1 ppm. At the same time, the EL shift of the same proton increases its fluctuation range from 0.23 to 0.32 ppm. It is worth noting that the shift differences can result in both increased shielding (e.g. EL shifts of H3′ and H2′, and SOL of H2′) or increased deshielding (RC of both H2′ and H3′) depending on the local geometry of the proton. Puckering of a ribose ring of course has a large effect on the local terms (eq 1) of the proton chemical shift. *Ab initio* calculations of the absolute shielding of ribose protons have shown that the shift difference for S and N conformers are significant and range from 0.7 ppm for H1′ to 0.1 ppm for H3′ protons.[17]

(32) Saenger, W. *Principles of nucleic acid structure*; Springer-Verlag: New York, 1984.

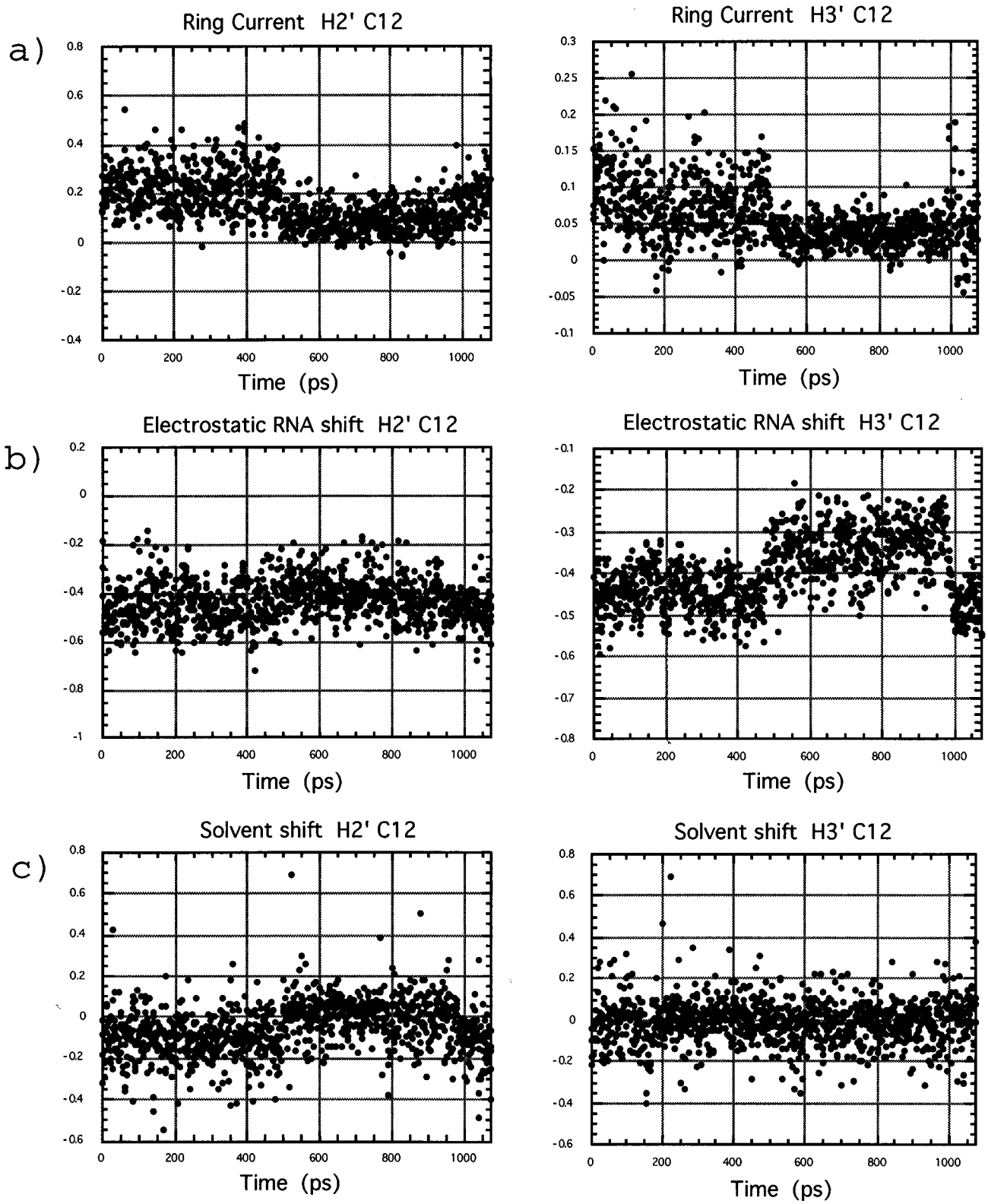

Figure 9. Time evolution of chemical shifts for protons involved in the ribose puckering of residue C12: (a) ring current shift, (b) intermolecular electrostatic shift, and (c) solvent shift of H2′ (left panels) and H3′ (right panels) protons. The change from C3′ endo to C2′ endo pucker occurred at 480 ps and the new conformation was retained for 500 ps.

Discussion

The values of δ_{loc}, A_{el}, B_{rc}, and C obtained from the fitting procedure led to several conclusions. First, the best agreement with the experimental data was obtained when the contributions of the solvent were excluded from the calculation. This means that the solvent effects are negligible for the aromatic nonexchangeable protons of the UUCG hairpin. If this is true in general, it implies that the calculation of chemical shifts for these protons can be done without the necessity of including the structure of the solvent, which is difficult to generate. Second, the value of parameter B_{rc} remained nearly constant and close to 1 during the fitting procedure, even when radically different values of calculated electrostatic effects were used (e.g. obtained with distance-dependent and distance-independent

dielectric functions). This implies that the ring current effects are being adequately represented by the existing approximation and parameters. Third, the intramolecular electrostatic effects gave a best fit with an effective dielectric constant of 2.1 (A_{el} = 0.474). This value is similar to dielectric constants measured in simple aromatic compounds and protein interiors.[31] It must be stressed that these conclusions are based on a calculation involving a small set of measured shifts—20 shifts were fit to 10 parameters—from a single RNA molecule. A much wider set of molecules must be studied to allow more general conclusions.

The time fluctuations of proton chemical shifts are caused by motions of RNA which occur during the simulation. Different dynamic events contribute to the chemical shift evolution according to their spatial extent and the frequency of occurrence. The time scale of our simulation allowed us to study the averaging effects of only fast events like bond vibrations, solvent rearrangement, and small magnitude helix bending.[33] Most of the shift fluctuations due to these motions are quickly averaged to a single unique value within the first 100 ps of the simulation (Figure 4). Although the averaging process is fast, the magnitudes of shift oscillations are large, and it is important to sample RNA conformations frequently in order to obtain correct time-averaged values. Lower frequency motions represented by a single change in ribose sugar pucker also create large differences in calculated chemical shifts but are too slow to average properly in our experiment. In nucleic acids ribose puckering is a frequent event which can be easily detected by H1′-H2′ *J*-coupling values.[34] NMR data for the UUCG hairpin shows that at least four nucleotides G1, U6, C7, and C12 contain the ribose ring in a mixed equilibrium between C3′ and C2′ endo conformations.[30] Since the ring puckering occurred only once for a C12 residue, it is clear that this process is statistically underrepresented on the nanosecond time scale, and the correctly averaged shift values cannot be obtained from this length of simulation. Longer molecular dynamics simulation times on the order of 10 ns are likely to give a more satisfactory description of ribose puckering in RNA. Finally, many internal motions of large amplitudes like the opening of Watson—Crick base pairs and helix bending are completed in microseconds. These and other events affect measured chemical shifts but cannot yet be represented in a realistic molecular dynamics simulation.

We found that the calculated values of the time-averaged shifts are different from shifts calculated from an NMR-derived structure (Figure 8). Protons exhibiting large shift fluctuations are most likely to give incorrect shift values when calculated from a single snapshot. This discrepancy suggests that a single, energy-minimized NMR structure is not adequate for the correct calculation of observed chemical shifts. We suggest that in the absence of a molecular dynamics trajectory, the calculation of chemical shifts should be done on a large family of converged NMR structures which provides a better representation of the average solution structure. Chemical shift values obtained in this way could then be used in structure refinement.

Our calculations reproduce the measured shifts of nonexchangeable aromatic protons to ±0.13 ppm and are also in qualitative agreement with the trends observed in ribose protons' chemical shifts. For instance, calculated shift contributions can account for several unusually shifted protons in the loop residues. Besides the large upfield shift of H5″ C7 discussed in the results section, calculated shifts of H1′ G9 and H3′ G8 are also in agreement with experimental data. H1′ G9 resonates at 4.38 ppm, which is about 1.4 ppm upfield from other H1′ protons and H3′ G8 is shifted 1.0 ppm downfield from other H3′ protons. The calculated shifts for these hydrogens are +0.9 and −0.5 ppm different from the calculated average shifts of H1′ and H3′ protons, respectively. Both of these shifts are dominated by large ring current effects.

Clearly there is a need for more accurate methods for calculating chemical shifts. The distinction between local and nonlocal effects (eq 1) assumes that a molecule can be approximately treated as a sum of groups with negligible electron exchange between them. The local effects operate within a group; the nonlocal effects are between groups. The nonlocal effects can be further divided into two types: magnetic field effects and electric field effects. To calculate the induced magnetic field at a nucleus we use the magnetic susceptibility tensors of the surrounding groups. These can be approximated by bond magnetic susceptibility tensors or by ring currents for aromatic rings. The induced magnetic field simply adds to the magnetic field at each nucleus so calculation of the nonlocal magnetic effects are independent of whether the nucleus is ^{1}H, ^{13}C, ^{15}N, etc. The electric field effects, however, require different parameters for different nuclei and different bonds. Once the electric field is calculated, its effect on the electron distribution around a nucleus is required. The simple Buckingham equation[7] for protons can not be used for other nuclei, and the coefficient *A* should in principle depend on the atom the proton is bonded to. The high sensitivity of chemical shifts to small changes in molecular conformations makes it important to improve the ability to calculate chemical shifts and to use measured shifts in determining molecular structure.

Acknowledgment. This work was supported by NIH Grant GM 10840 (I.T.), NIH Grant CA-25644 (P.A.K.), and Department of Energy Grant DE-FG03-86ER60406 (I.T.). J.L.M. is grateful for support from the NIH Grant GM07175 and the American Foundation for Pharmaceutical Education.

JA9625945

(33) McCammon, A. J.; Harvey, S. C. *Dynamics of proteins and nucleic acids*; University Press: Cambridge, 1987; p 234.

(34) Altona, C. *Recl. Trav. Chim. Pays.-Bas.* **1982**, *101*, 413—433.